










HATS: A Ground-Based Telescope to Explore the THz Domain

C. Guillermo Giménez de Castro^{1,2}  ·
Jean-Pierre Raulin¹  · Adriana Valio¹  ·
Guilherme Alaia¹ · Vinicius Alvarenga³ ·
Emilio Carlos Bortolucci⁴  ·
Silvia Helena Fernandes¹  ·
Carlos Francile⁵ · Tiago Giorgetti¹ ·
Amauri Shossei Kudaka¹  ·
Fernando Marcelo López¹  ·
Rogério Marcon^{6,7} · Adolfo Marun⁸  ·
Márcio Zaquela⁹ 

© Springer

✉ C.G. Giménez de Castro
guigue@craam.mackenzie.br

- ¹ Centro de Rádio Astronomia e Astrofísica Mackenzie, Escola de Engenharia, Universidade Presbiteriana Mackenzie, Rua da Consolação 896, 01302-907, São Paulo, Brazil.
- ² Instituto e Astronomía y Física del Espacio, CONICET-UBA, CC. 67 Suc. 28, 1428, Buenos Aires, Argentina.
- ³ Mackgraphe, Escola de Engenharia, Universidade Presbiteriana Mackenzie, Rua da Consolação 896, 01302-907, São Paulo, Brazil.
- ⁴ Centro de Componentes Semicondutores e Nanotecnologias, Unicamp, Campinas, Brazil.
- ⁵ Observatorio Astronómico Félix Aguilar, Universidad Nacional de San Juan, San Juan, Argentina.
- ⁶ Instituto de Física Gleb Wataghin, Universidade Estadual de Campinas, Campinas, SP, Brazil.
- ⁷ Observatório Solar Bernard Lyot, Campinas, SP, Brazil.
- ⁸ Instituto de Ciencias Astronómicas, de la Tierra y del Espacio, CONICET-UNSJ, San Juan, Argentina.
- ⁹ Advanced Embedded R&D Lab, São Paulo, Brazil.

Abstract The almost unexplored frequency window from submillimeter to mid-infrared (mid-IR) may bring new clues about the particle acceleration and transport processes and the atmospheric thermal response during solar flares. Because of its technical complexity and the special atmospheric environment needed, observations at these frequencies are very sparse. The High Altitude THz Solar Photometer (HATS) is a full-Sun ground-based telescope designed to observe the continuum from the submillimeter to the mid-IR. It has a 457-mm spherical mirror with the sensor in its primary focus. The sensor is a Golay cell with high sensitivity in a very wide frequency range. The telescope has a polar mount, and a custom-built data acquisition system based on a 32 ksamples per second, 24 bits (72 dB dynamic range), 8 channels analog-to-digital board. Changing only the composition of the low- and band-pass filters in front of the Golay cell, the telescope can be setup to detect very different frequency bands; making the instrument very versatile. In this article we describe the telescope characteristics and its development status. Moreover, we give estimates of the expected fluxes during flares.

1. Introduction

Until the installation of the Solar Submillimeter Telescope (SST: Kaufmann *et al.*, 2008) in 1999, flare radiation in the submillimeter wavelength range was almost unexplored. SST has shown that the gyrosynchrotron emission model applied for microwaves (Bastian, Benz, and Gary, 1998) does not always fit in the submillimeter wavelength range observations. Indeed, Kaufmann *et al.* (2004) have shown for the first time a flare with a submillimeter spectrum inverting the tendency to decrease with frequency as expected for the optically thin gyrosynchrotron emission (Ramaty, 1969). More observations (Lüthi, Magun, and Miller, 2004; Silva *et al.*, 2007; Kaufmann *et al.*, 2009) confirmed the existence of these new *THz-events*. A review of the observed flares at the submillimeter range can be found in Krucker *et al.* (2013) and Fernandes *et al.* (2017). It is clear, that there is not one unique mechanism that can explain the emission at this frequency range, and that observations at higher frequencies are needed to complete the observational diagnostics.

However, the nearer the THz limit, the higher the atmospheric opacity and the costs associated to build and operate such facility. At the other end of the THz range, the infrared (IR), commercial cameras at the focus of small telescopes can be used to image flares with a relatively good sensitivity. Kaufmann *et al.* (2013) have shown at the mid-IR frequency of 30 THz (10 μm) strong flux densities during an X-class flare which are temporally coincident with the white-light flare. The origin of this emission was interpreted by Trottet *et al.* (2015) as the atmospheric thermal response to the energy deposited by impinging particles (electrons and ions) over the chromosphere. Later on Penn *et al.* (2016) showed that weaker flares, in the Geostationary Operational Environmental Satellite (GOES) class C7, also produce mid-IR radiation.

The IR emission mechanism during flares was first described by Ohki and Hudson (1975) who related it with the appearance of white-light flares and suggested two different sources: a chromospheric optically thin thermal bremsstrahlung and/or a photospheric optically thick black body emission dominated by the H⁻ opacity. Kašparová *et al.* (2009) and Simões *et al.* (2017) arrived to similar conclusions modelling the IR to mm-waves emission starting from a non-perturbed atmosphere and calculating the ionization produced by the precipitating electrons via hydrodynamics simulations; while Heinzel and Avrett (2012) reached similar results using Machado *et al.* (1980) and Mauas, Machado, and Avrett (1990) semi-empirical flare models. Moreover, Kašparová *et al.* (2009) showed that the thermal radiation is modulated by the beam flux and can be composed of very fast pulses. Simões *et al.* (2017) found that the near IR continuum is optically thin, as shown by Penn *et al.* (2016) with observations at 5.2 and 8.2 μm and by Trottet *et al.* (2015) at 10 μm . Moreover, Simões showed that for $\lambda \simeq 50 \mu\text{m}$ the emission becomes optically thick. These results are, however, model-dependent, therefore a better observational spectral coverage between the millimeter range and IR is needed to properly assess the theoretical models, characterize the radiation mechanism, and reveal the process of energy transport from the energy release site to the radiation emission location. Since the observation of powerful flares in Proxima Centauri at 0.233 THz (MacGregor *et al.*, 2018; MacGregor, Osten, and Hughes, 2020) the interest in this spectral range is not no longer just relevant to the Sun.

The Solar-T balloon experiment (Kaufmann *et al.*, 2014) was the first instrument designed to observe the Sun in the THz range. This article describes new ground-based telescopes for observations at the submillimeter and mid-IR wavelengths similar to Solar-T. In this article we explain the particularities of these new facilities, the expected fluxes, and put them in the context of previous works.

2. HATS Description

The telescope concept is described by Kaufmann *et al.* (2014); it is based on a single opto-acoustic photometer (a Golay cell) at the focus of a reflector telescope. The optical system creates an image of the Sun with the size of the entrance cone of the Golay cell, i.e. even with a large mirror and only one-pixel sensor, the system behaves like a full-Sun instrument. This concept was applied in the Solar-T balloon experiment that flew over Antarctica for two weeks in January 2016 with a couple of Cassegrain telescopes and receivers for 3 and 7 THz respectively.

HATS is a ground-based telescope that uses the same concept but is designed to operate from the submillimeter to the mid-IR. It is a prime focus system, with a spherical mirror. To reduce the IR radiation the mirror is roughened. It has a diameter $\phi = 457 \text{ mm}$ and a focal distance $f = 1007 \text{ mm}$ (Figure 1), therefore

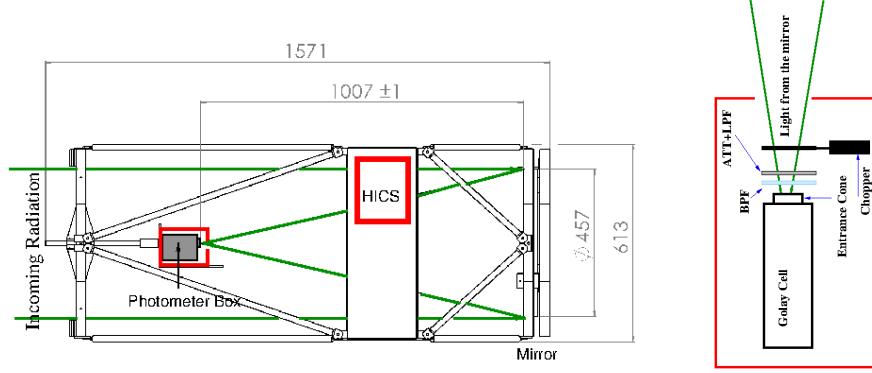


Figure 1. *Left:* HATS general diagram, a prime focus system composed of a 457 mm spherical mirror, the photometer box, and the data acquisition computer HATS Interface and Control System (HICS). Dimensions are in mm. *Right:* The Photometer box with the chopper, attenuators (ATT), low-pass (LPF) and band-pass (BPF) filters. Green lines represent light rays.

the optical solar disk will produce an image at the focus with diameters between 9.21 mm (aphelion), 9.52 mm (perihelion) and 9.36 mm in average, all of them smaller than the photometer entrance cone which has a diameter ≥ 10 mm. The mirror was roughened using carborundum $1.25 \mu\text{m}$ (E10); its reflectance $R(\lambda)$ in function of wavelength yields $R \simeq 1$ and $R \simeq 0.3$ for $\lambda = 300 \mu\text{m}$ and $\lambda = 20 \mu\text{m}$, respectively (Fernandes, 2013). The Golay cell is inside a box, with the chopper, low-pass filters, attenuators, and the frequency selector band-pass filter. The set of filters can be changed to select different wavelength ranges. Attenuators and low-pass filters are used to block $\lambda < 5 \mu\text{m}$ wavelengths and reduce the incoming power to the sensor maximum measurable power. Figure 1 shows diagrams of the telescope and the photometer box where the Golay cell, filters, and chopper are installed.

HATS was originally conceived as a robotic telescope observing at $\nu_o = 0.87 \text{ THz}$ and $\nu_o = 1.4 \text{ THz}$ or $\lambda_o = 344 \mu\text{m}$ and $\lambda_o = 214 \mu\text{m}$, respectively (Kaufmann *et al.*, 2015b). It has two metal-mesh band-pass filters placed in a rotating wheel with period $P \simeq 5 \text{ Hz}$ that also serves as a chopper. They were built at Centro de Componentes Semicondutores (CCS), a laboratory of the Universidade Estadual de Campinas (Unicamp) and tested at the Max Planck Institute für extraterrestrische Physik in Garching, Germany (Melo *et al.*, 2008). Filter characteristics are presented in Table 1. In order to minimize restrictions from atmospheric absorption, the telescope should be installed at a very high altitude (≥ 5000 meters above sea level (masl)) where the precipitable water vapor content (PWV) should be less than 1 mm during a large fraction of the year. Since such locations are generally isolated with limited infrastructure, like Solar-T, HATS should use satellite communication for data downloading and monitoring, electric power from solar panels and an intelligent radome that opens during observations and closes at night or when atmospheric conditions may damage the system.

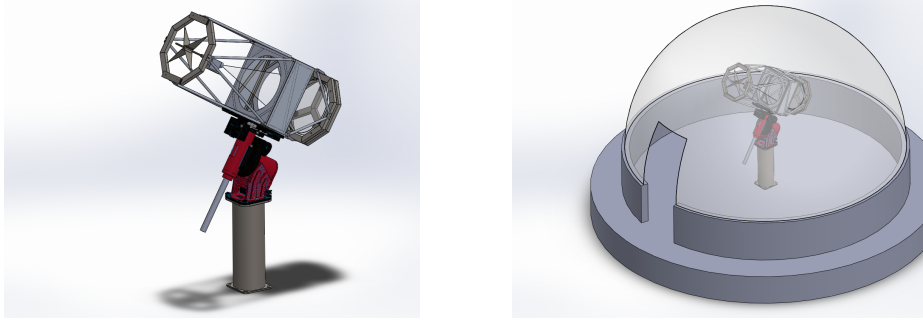


Figure 2. A projected 3D view of HATS-mir (left) and inside the polypropylene radome in park position, pointing to South (right).

While we look for a place where to install the THz telescope, we are working in a mid-IR version of HATS because the atmospheric opacity at this frequency is not very high at medium elevations, and therefore there are more candidates for the installation site. To distinguish between the different HATS setups we refer to the submillimeter version as the HATS-smm and the mid-IR as HATS-mir.

HATS-mir has a sensor with a central frequency $\nu_o = 15$ THz ($\lambda_o = 20 \mu\text{m}$), see Table 1. It will be installed at $\simeq 2300$ masl at the Observatorio Astronómico Félix Aguilar (OFA, Argentina) which will provide electric power and Internet connection; the telescope will be enclosed in a radome and manually operated from a control room. Figure 2 is a projected 3D view of HATS-mir including the radome. The telescope is made of aluminum bars, has lateral bays to accommodate auxiliary devices, is placed over a Paramount ME II equatorial mount and protected from the wind and dust by a translucent polypropylene semi-spherical radome 4.5 m wide standing over a 0.7 m high circular wall. The polypropylene material was chosen because it has a relatively high transmission ($\simeq 0.35$) at the observing frequency. The decision as to whether we will use a fork or a wheel chopper (in Figure 1 a fork chopper is represented) is still being evaluated. The band-pass filter is fabricated from thin metal foil with holes by the Saint Petersburg company Tydex, model BPF15.0-24, attenuators and low-pass filters are also fabricated by Tydex. We plan to stack together two band-pass filters to increase the side frequency rejection, Figure 3 shows the response in frequency of the set of filters. The responses of all components in the telescope light path are tested with a Fourier Transform Infrared Interferometer in the Centro de Pesquisas em Grafeno e Nanomateriais (Mackgraph) of the Universidade Presbiteriana Mackenzie, São Paulo, Brazil. Some of the optical system components may change until the telescope is finally installed, however, the total transmission η_{ν_o} should not change significantly because we can compensate using different optical attenuators.

Both HATS-mir and HATS-smm use a Tydex Golay cell GC-1T whose analog output is digitized using an AD7770 Analog Devices Inc. converter with 24 bits,

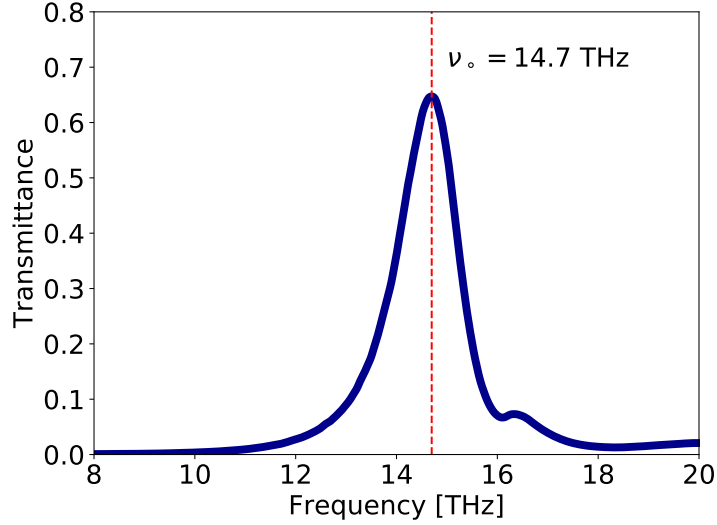


Figure 3. Transmittance of two stacked Tydex band-pass filters as a function of frequency.

Table 1. Characteristics of the band-pass filters.

| Origin | Wavelength [μm] | Frequency [THz] | Bandwidth [% of central Frequency] | Transmission [%] |
|--------|---------------------------------|--------------------|---------------------------------------|---------------------|
| CCS | 352 | 0.87 | 14.0 | 84 |
| Tydex† | 20.0 | 15.0 | 7.0 | 65 |

†: two stacked filters.

8 channels and 32 ksamples^{-1} . The converter is controlled with a ATMEL ATSAME-XPRO single board computer running a real time Linux operating system (freeRTOS): this ensemble is called the HATS Interface and Control System (HICS) and is installed in the telescope lateral bay (Figure 1). With a 24-bit analog-to-digital converter, we have a 72 dB dynamic range, which allows us to detect signals much weaker than the sensor sensitivity. The HATS Operation, Monitoring and Storage (HOMS) is a desktop computer installed at the control room running the telescope control software, connected through Ethernet to HICS and the Paramount mount. The mount has a proprietary control software called TheSkyX. While this software has a graphical user interface, remote commands, written in Javascript, can be sent to the mount through an Ethernet connection. Global Positioning System (GPS) receiver is used to set HOMS time, that runs an Network Time Protocol (NTP) server to synchronize the computers in the network. Data are read at a 1 kHz rate, and transferred to HOMS where it is window-Fourier transformed. A peak around the chopper frequency should show up, therefore, the window of the Fourier transforms defines the signal time resolution: from 256 to 1024 ms. The sensor response as a function of temperature is calibrated by comparing the output signal against a black-body

source, resulting in a linear relationship between voltage and temperature which is later used for data calibration (Kaufmann *et al.*, 2014).

3. Expected Signal Input

Here we compute the expected incoming power for $\nu = 0.87$ THz and 15 THz. There are three sources of emission: the quiet Sun (QS), the flare (FL), and the sky (SK), the observed flux density F_{obs} will then be given by

$$F_{\text{obs}} = F_{\text{FL}} + F_{\text{QS}} + F_{\text{SK}} . \quad (1)$$

We will analyze each term separately. First the QS; since the Sun has a brightness temperature between 4500 and 5500 K for the observing range of the telescope, the Raleigh-Jeans (RJ) approximation is valid for the submillimetric to the mid-IR range. Therefore the expected flux density above the atmosphere is

$$F_{\text{QS}} = \frac{2k_{\text{B}}T_{\odot}\nu_{\odot}^2}{c^2}\Omega_{\odot} \quad [\text{Wm}^{-2}\text{Hz}^{-1}] , \quad (2)$$

where k_{B} is the Boltzmann constant, c the speed of light in vacuum, T_{\odot} is the QS temperature for the frequency ν_{\odot} and Ω_{\odot} is the Sun solid angle from Earth, which is smaller than the telescope field of view solid angle Ω_{t} . The sky contribution to the flux density is, on the other hand,

$$F_{\text{SK}} = \frac{2k_{\text{B}}T_{\text{SK}}\nu_{\odot}^2}{c^2}\Omega_{\text{t}}(1 - e^{-\tau_{\nu_{\odot}}\zeta}) \quad [\text{Wm}^{-2}\text{Hz}^{-1}] , \quad (3)$$

where T_{SK} is the sky brightness temperature, $\tau_{\nu_{\odot}}$ the zenith optical depth for the frequency ν_{\odot} , and $\zeta = 1/\sin(\text{elevation})$, the airmass.

Estimating F_{FL} is model dependent. For instance, we can use Simões *et al.* (2017) to deduce brightness temperature for a *thermal* flare. However we prefer to determine the minimum flux density that could be detected. This will be addressed in the next section.

F_{QS} and F_{FL} are attenuated by the atmosphere by a factor

$$\mathcal{A}(\nu) = e^{-\tau_{\nu_{\odot}}\zeta} . \quad (4)$$

We set in this analysis $\zeta = 1.71$ which corresponds to the mean value for elevations between 10° and 85° . Values for $\tau_{\nu_{\odot}}$ are strongly dependent on the observing site. We consider in this work two different absorption scenarios: *i*) a mid-altitude site at 2500 masl for $\nu_{\odot} = 15$ THz and *ii*) a high-altitude site at 5000 masl for $\nu_{\odot} = 0.87$ THz. The mid-IR camera report of the Gran Telescopio Canarias (<http://www.gtc.iac.es/instruments/canaricam/MIR.php>, accessed on 2019-11-19) uses Atmospheric Transmission (ATRAN) models for atmospheric transmission in the range $300 \geq \nu \geq 12$ THz at a mid-altitude site. Results imply that the transmission is weakly dependent on PWV, for a range between 2.3 to 10 mm,

Table 2. Table with model parameters. †: Righini and Simon (1976), §: Simões *et al.* (2017).

| Telescope Setup | ν_o (THz) | T_\odot (K) | T_{SK} (K) | τ | ζ | η_{ν_o} | A_{surf} (m ²) |
|--------------------|------------------|-------------------|------------------------|--------|---------|----------------------|--|
| HATS-smm | 0.87 | 4500 [†] | 290 | 1.0 | 1.71 | 7.1×10^{-1} | 0.164 |
| HATS-mir | 15.0 | 5600 [§] | 290 | 0.3 | 1.71 | 1.1×10^{-2} | 0.164 |

yielding a mean value $\tau_\nu = 0.35$ for $12 \leq \nu \leq 20$ THz. The PWV range used for the ATRAN simulations is similar to the range at the Complejo Astronómico El Leoncito (CASLEO) observatory (Cassiano *et al.*, 2018), which is 5 km away from OAFA where HATS-mir will be installed.

On the other hand, the submillimeter wavelengths are strongly dependent on PWV. Using the Atmospheric Transmission at Microwaves (ATM) model (Pardo, Cernicharo, and Serabyn, 2001) and the statistical analysis of the optical depth at 210 GHz for the Alto Chorrillo site (4850 masl, Salta, Argentina, Bareilles *et al.*, 2011), we obtain a $\tau_\nu \leq 1.0$ at $\nu = 0.87$ THz for around 30 days per year.

To get the total power received by the photometer P_{ν_o} , we need to multiply by the mirror surface area A_{surf} , the product of all of the blocking, transmission, and reflection factors along the optical path η_{ν_o} and convolve with the band-pass filter response $f_{\text{PB}}(\nu)$, i.e.

$$P_{\nu_o} = \frac{A_{\text{surf}} \eta_{\nu_o}}{2} \int F_{\text{obs}}(\nu) f_{\text{BP}}(\nu) d\nu, \quad F_{\text{obs}} = (F_{\text{FL}} + F_{\text{QS}}) \mathcal{A}(\nu) + F_{\text{SK}}. \quad (5)$$

Table 2 summarizes the different parameters used in these simulations. The total transmission factor η_{ν_o} for HATS-mir is the multiplication of the polypropylene radome transmission (0.35), the mirror reflectivity (0.3), the fraction of mirror light converging to the sensor because of the photometer box blocking ($\simeq 0.88$), and the chopper (0.61 for a fork chopper, 1.0 for a wheel chopper). In case the incoming power is still larger than the Golay cell manufacturer recommended maximum detected power (10^{-5} W) attenuators must be added in the optical path.

3.1. Flare Detectability

The main purpose of HATS is to characterize flares in the THz to mid-IR range, and with this aim it was designed. To estimate the power produced by a flare in the photometer we will proceed from the Golay cell noise and convert it to flux density. The photometer has a typical noise equivalent power $\text{NEP} = 1.4 \times 10^{-4} \mu\text{W Hz}^{-1/2}$. The noise power is determined multiplying the NEP by the square root of the modulation frequency

$$P_{\text{noise}} = \text{NEP} \sqrt{f_{\text{chopper}}} = 1.4 \times 10^{-4} \times \sqrt{15} = 5.4 \times 10^{-4} \mu\text{W}, \quad (6)$$

Table 3. Expected minimum flare flux density detectable for the different HATS setups.

| Telescope Setup | ν_o | $\Delta_{\text{eff}}\nu$ (THz) | P_{min} | Quiet Sun (μW) | Sky | $\mathcal{A}(\nu)$ | F_{min} (10^3 SFU) |
|-----------------|---------|-----------------------------------|------------------|--------------------------------|-------|--------------------|-----------------------------------|
| HATS-smm | 0.87 | 0.11 | 0.0016 | 0.077 | 0.001 | 0.18 | 14 |
| HATS-mir | 15.0 | 1.19 | 0.0016 | 9.66 | 0.34 | 0.60 | 23 |

where $f_{\text{chopper}} = 15$ Hz is the typical chopper frequency. By definition P_{noise} is the incoming power on the detector that produces an output equal to the root mean square (RMS) noise. To be able to detect an external signal over noise we will assume a minimum incoming power $P_{\text{min}} = 3 \times P_{\text{noise}} = 1.6 \times 10^{-3} \mu\text{W}$. Then, the minimum flare flux density detectable is

$$F_{\text{min}} = \frac{2 P_{\text{min}}}{A_{\text{surf}}} \frac{1}{\mathcal{A}(\nu)} \frac{1}{\eta_{\nu_o}} \frac{1}{\Delta_{\text{eff}}\nu}, \quad \Delta_{\text{eff}}\nu = \int f_{\text{BP}}(\nu) d\nu, \quad (7)$$

$\Delta_{\text{eff}}\nu$ is the filter-averaged frequency range of the band-pass filter. Table 3 shows the expected minimum detectable flux densities for HATS-smm and HATS-mir. We included in the table the power produced by the quiet Sun and the sky (the total incoming power should be $\leq 10 \mu\text{W}$). We note that the dynamic range needed to detect a flare is

$$DR = 10 \log_{10} \left(\frac{P_{\text{total}}}{P_{\text{min}}} \right), \quad P_{\text{Total}} = P_{\text{min}} + P_{\text{QS}} + P_{\text{sky}}.$$

Replacing P_{Total} and P_{min} from Table 3 we get $DR_{\text{mir}} = 38$ dB and $DR_{\text{smm}} = 24$ dB for HATS-mir and HATS-smm, respectively, which are smaller than the DR 72 dB of the acquisition system (Section 2).

4. Discussion

The minimum detectable flux densities derived from the telescope average observing configurations are of the order of $10 - 25 \times 10^3$ SFU. Since there are no previous reports of flares at the frequencies of HATS operation, we will compare our estimates with observations at frequencies near those of HATS.

In the mid-IR range, Kaufmann *et al.* (2015a) reported flux densities recorded with a 30 THz ($10 \mu\text{m}$) camera as high as 35×10^3 SFU for an X2 event (SOL2014-10-27T14:22), the highest ever reported. Other works also give values of the order of 10^4 SFU, although more moderate (see Kaufmann *et al.*, 2013; Giménez de Castro *et al.*, 2018). While these events are strong flares (M8 and X9 GOES class), Penn *et al.* (2016) presented observations at 5.2 and 8.2 μm during the M7 class flare SOL2014-09-24T17:50 with maximum flux densities < 1000 SFU,

that would not be detected by HATS-mir.

On the other hand, from theoretical simulations we can reasonably expect an excess brightness temperature $T_{fl} \simeq 3 \times 10^3$ K at $\nu \simeq 15$ THz produced by accelerated electrons heating the chromosphere (Simões *et al.*, 2017). Considering an average thermal source extending over a surface $A_{\text{source}} = 6 \times 10^{18}$ cm², corresponding to a solid angle $\Omega_s \simeq 3 \times 10^{-8}$ str, the flux density produced by this thermal source would be $F_x = 59 \times 10^3$ SFU, and therefore, detectable by HATS-mir. The main limitation to increase HATS-mir sensitivity is the quiet Sun background emission and, to a lesser extent, the sky radiation: the minimum flare detectable power is a thousandth of the background power over the photometer. The same large mirror that allows us to gather enough flux from the tiny flare to detect it, gathers also the strong mid-IR emission coming from the full quiet Sun.

In the sub-millimeter range, the most intense flare already detected, SOL2003-11-02T17:17, an X8 GOES class flare, had a flux density peak $F_x \simeq 65 \times 10^4$ SFU at 0.4 THz (Silva *et al.*, 2007). Since its submillimeter spectrum increases from 0.2 toward 0.4 THz, it is expected that the flux density at 0.87 THz should be even higher. We note, however, that this was a rather unusual event with an extremely steep submillimeter spectral index. Another submillimeter event where the intensity increases towards the highest frequencies is SOL2013-11-04T19:43 (Kaufmann *et al.*, 2004). During peak time, the submillimeter spectral index

$$\alpha = \frac{\log\left(\frac{F_{0.4}}{F_{0.21}}\right)}{\log\left(\frac{0.4}{0.21}\right)} \simeq 0.8 .$$

If the same spectral index is applied to the flux between 0.4 and 0.87 THz we obtain

$$F_{0.87} = F_{0.4} \left(\frac{0.87}{0.4}\right)^{0.8} \simeq 36 \times 10^3 \text{ SFU} .$$

While these numbers may be encouraging, we have to remember that just a few submillimeter flares had fluxes $> 10^4$ SFU in the last two solar cycles (Krucker *et al.*, 2013; Fernandes *et al.*, 2017). The high atmospheric opacity is the main obstacle at 0.87 THz – if we consider $\tau_\nu = 0.5$ and $\zeta = 1.01$ (elevation=80°) the minimum detectable flux density drops to $\simeq 4000$ SFU. However, such a low atmospheric optical depth is expected for only a few days per year in most of the installation sites already analyzed.

HATS-mir is under construction at Centro de Rádio Astronomia e Astrofísica Mackenzie (CRAAM, São Paulo, Brazil) and will be transported and installed in the OAFa observatory in June 2020. First light is expected for September 2020. There is still no provision for the construction of HATS-smm. Both HATS setups, when operating, will bring flare data from yet unexplored frequencies. These new frequency windows will complement the millimeter observations of the Polarization Emission of Millimeter Activity at the Sun (POEMAS, for

0.045 and 0.090 THz, Valio *et al.*, 2013), the submillimeter range of the SST, and the mid-IR of the 30 THz cameras. As solar dedicated telescopes, they will create a data base of flares to constrain theoretical models for the flare energy transport to the chromosphere/photosphere. We remark that these are unique instruments in this frequency range, since only the Atacama Large Millimeter Array (ALMA) can observe solar flares at submillimeter wavelengths, however with very limited observing times because of its high demand.

Acknowledgments C.G. Giménez de Castro and J.-P. Raulin acknowledge CNPq (contracts 305203/2016-9 and 312066/2016-3). The research leading to these results has received funding from CAPES grant 88881.310386/2018-01, FAPESP grant 2013/24155-3, and the US Air Force Office for Scientific Research (AFOSR) grant FA9550-16-1-0072.

Disclosure of Potential Conflicts of Interest

The authors declare that they have no conflicts of interest.

References

- Bareilles, F., Morras, R., Hauscarriaga, F.P., Guarrera, L., Arnal, E.M., Lepine, J.R.D.: 2011, Comparación entre los sitios de LLAMA y APEX. In: *Bol. Asoc. Arg. de Astron.* **54**.
- Bastian, T.S., Benz, A.O., Gary, D.E.: 1998, Radio Emission from Solar Flares. *Ann. Rev. Astron. Astr.* **36**, 131. DOI. ADS.
- Cassiano, M.M., Cornejo Espinoza, D., Raulin, J.-P., Giménez de Castro, C.G.: 2018, Precipitable water vapor and 212 GHz atmospheric optical depth correlation at El Leoncito site. *J. Atmos. Sol-Terr. Phys.* **168**, 32. DOI. ADS.
- Fernandes, L.O.T.: 2013, Desenvolvimento de fotômetros thz para observação de explosões solares. Master's thesis, Unicamp. Link: <http://repositorio.unicamp.br/jspui/handle/REPOSIP/259238>.
- Fernandes, L.O.T., Kaufmann, P., Correia, E., Giménez de Castro, C.G., Kudaka, A.S., Marun, A., Pereyra, P., Raulin, J.-P., Valio, A.B.M.: 2017, Spectral Trends of Solar Bursts at Sub-THz Frequencies. *Solar Phys.* **292**, 21. DOI. ADS.
- Giménez de Castro, C.G., Raulin, J.-P., Valle Silva, J.F., Simões, P.J.A., Kudaka, A.S., Valio, A.: 2018, The 6 September 2017 X9 Super Flare Observed From Submillimeter to Mid-IR. *Space Weather* **16**(9), 1261. DOI. ADS.
- Heinzel, P., Avrett, E.H.: 2012, Optical-to-Radio Continua in Solar Flares. *Solar Phys.* **277**, 31. DOI. ADS.
- Kaufmann, P., Raulin, J.-P., de Castro, C.G.G., Levato, H., Gary, D.E., Costa, J.E.R., Marun, A., Pereyra, P., Silva, A.V.R., Correia, E.: 2004, A New Solar Burst Spectral Component Emitting Only in the Terahertz Range. *Astrophys. J. Lett.* **603**(2), L121. DOI. ADS.
- Kaufmann, P., Levato, H., Cassiano, M.M., Correia, E., Costa, J.E.R., Giménez de Castro, C.G., Godoy, R., Kingsley, R.K., Kingsley, J.S., Kudaka, A.S., Marcon, R., Martin, R., Marun, A., Melo, A.M., Pereyra, P., Raulin, J.-P., Rose, T., Silva Valio, A., Walber, A., Wallace, P., Yakubovich, A., Zakia, M.B.: 2008, New telescopes for ground-based solar observations at submillimeter and mid-infrared. In: *Society of Photo-Optical Instrumentation Engineers (SPIE) Conference Series* **7012**. DOI. ADS.
- Kaufmann, P., Trottet, G., Giménez de Castro, C.G., Raulin, J.-P., Krucker, S., Shih, A.Y., Levato, H.: 2009, Sub-terahertz, Microwaves and High Energy Emissions During the 6 December 2006 Flare, at 18:40 UT. *Solar Phys.* **255**(1), 131. DOI. ADS.

- Kaufmann, P., White, S.M., Freeland, S.L., Marcon, R., Fernandes, L.O.T., Kudaka, A.S., de Souza, R.V., Aballay, J.L., Fernandez, G., Godoy, R., Marun, A., Valio, A., Raulin, J.-P., Giménez de Castro, C.G.: 2013, A Bright Impulsive Solar Burst Detected at 30 THz. *Astrophys. J.* **768**, 134. DOI. ADS.
- Kaufmann, P., Marcon, R., Abrantes, A., Bortolucci, E.C., T. Fernandes, L.O., Kropotov, G.I., Kudaka, A.S., Machado, N., Marun, A., Nikolaev, V., Silva, A., da Silva, C.S., Timofeevsky, A.: 2014, THz photometers for solar flare observations from space. *Exp. Astron.* **37**(3), 579. DOI. ADS.
- Kaufmann, P., White, S.M., Marcon, R., Kudaka, A.S., Cabezas, D.P., Cassiano, M.M., Francile, C., Fernandes, L.O.T., Hidalgo Ramirez, R.F., Luoni, M., Marun, A., Pereyra, P., Souza, R.V.: 2015a, Bright 30 THz impulsive solar bursts. *Journal of Geophysical Research (Space Physics)* **120**, 4155. DOI. ADS.
- Kaufmann, P., Abrantes, A., Bortolucci, E.C., Fernandes, L.O.T., I., K.G., Kudaka, A.S., Machado, N., Marcon, R., Nikolaev, V., Timofeevsky, A.: 2015b, Space and ground-based new tools for thz solar flare observations. In: *Proceedings of the 26th International Symposium on Space Terahertz Technology, ISSTT 2015*. Link: <https://www.cfa.harvard.edu/events/2015/isstt2015/proceedings/>.
- Kašparová, J., Heinzel, P., Karlický, M., Moravec, Z., Varady, M.: 2009, Far-IR and Radio Thermal Continua in Solar Flares. *Cent. Europ. Astrophys. Bull.* **33**, 309. ADS.
- Krucker, S., Giménez de Castro, C.G., Hudson, H.S., Trotter, G., Bastian, T.S., Hales, A.S., Kašparová, J., Klein, K.-L., Kretschmar, M., Lüthi, T., Mackinnon, A., Pohjolainen, S., White, S.M.: 2013, Solar flares at submillimeter wavelengths. *Astron. Astrophys. Rev.* **21**, 58. DOI. ADS.
- Lüthi, T., Magun, A., Miller, M.: 2004, First observation of a solar X-class flare in the submillimeter range with KOSMA. *Astron. Astrophys.* **415**, 1123. DOI. ADS.
- MacGregor, A.M., Osten, R.A., Hughes, A.M.: 2020, Properties of M Dwarf Flares at Millimeter Wavelengths. *Astrophys. J.* **891**(1), 80. DOI. ADS.
- MacGregor, M.A., Weinberger, A.J., Wilner, D.J., Kowalski, A.F., Cranmer, S.R.: 2018, Detection of a Millimeter Flare from Proxima Centauri. *Astrophys. J. Lett.* **855**(1), L2. DOI. ADS.
- Machado, M.E., Avrett, E.H., Vernazza, J.E., Noyes, R.W.: 1980, Semiempirical models of chromospheric flare regions. *Astrophys. J.* **242**, 336. DOI. ADS.
- Mauas, P.J.D., Machado, M.E., Avrett, E.H.: 1990, The white-light flare of 1982 June 15 - Models. *Astrophys. J.* **360**, 715. DOI. ADS.
- Melo, A.M., Kornberg, M.A., Kaufmann, P., Piazzetta, M.H., Bortolucci, E.C., Zakia, M.B., Bauer, O.H., Poglitsch, A., Alves da Silva, A.M.P.: 2008, Metal mesh resonant filters for terahertz frequencies. *App. Optics* **47**(32), 6064. DOI. ADS.
- Ohki, K., Hudson, H.S.: 1975, The solar-flare infrared continuum. *Solar Phys.* **43**, 405. ADS.
- Pardo, J.R., Cernicharo, J., Serabyn, E.: 2001, Atmospheric transmission at microwaves (ATM): an improved model for millimeter/submillimeter applications. *IEEE Trans. on Antenn. Propag.* **49**(12), 1683. DOI. ADS.
- Penn, M., Krucker, S., Hudson, H., Jhabvala, M., Jennings, D., Lunsford, A., Kaufmann, P.: 2016, Spectral and Imaging Observations of a White-light Solar Flare in the Mid-infrared. *Astrophys. J. Lett.* **819**, L30. DOI. ADS.
- Ramaty, R.: 1969, Gyrosynchrotron Emission and Absorption in a Magnetoactive Plasma. *Astrophys. J.* **158**, 753. DOI. ADS.
- Righini, G., Simon, M.: 1976, Solar brightness temperature distribution at 350 and 450 microns. *Astrophys. J. Lett.* **203**, L95. DOI. ADS.
- Silva, A.V.R., Share, G.H., Murphy, R.J., Costa, J.E.R., de Castro, C.G.G., Raulin, J.-P., Kaufmann, P.: 2007, Evidence that Synchrotron Emission from Nonthermal Electrons Produces the Increasing Submillimeter Spectral Component in Solar Flares. *Solar Phys.* **245**, 311. DOI. ADS.
- Simões, P.J.A., Kerr, G.S., Fletcher, L., Hudson, H.S., Giménez de Castro, C.G., Penn, M.: 2017, Formation of the thermal infrared continuum in solar flares. *Astron. Astrophys.* **605**, A125. DOI. ADS.
- Trotter, G., Raulin, J.-P., Mackinnon, A., Giménez de Castro, G., Simões, P.J.A., Cabezas, D., de La Luz, V., Luoni, M., Kaufmann, P.: 2015, Origin of the 30 THz Emission Detected During the Solar Flare on 2012 March 13 at 17:20 UT. *Solar Phys.* **290**, 2809. DOI. ADS.
- Valio, A., Kaufmann, P., Giménez de Castro, C.G., Raulin, J.-P., Fernandes, L.O.T., Marun, A.: 2013, Polarization Emission of Millimeter Activity at the Sun (POEMAS): New Circular

Polarization Solar Telescopes at Two Millimeter Wavelength Ranges. *Solar Phys.* **283**, 651.
DOI. ADS.